EUROPEAN ORGANIZATION FOR NUCLEAR RESEARCH

L3 Note 2754
June 26, 2002

Preliminary Results on the Measurement of Mass and Width of the W Boson at LEP

The L3 Collaboration

Abstract

We report on measurements of the mass and total decay width of the W boson with the L3 detector at LEP. W-pair events produced in e^+e^- interactions between 161 GeV and 208 GeV centre-of-mass energy are selected in a data sample corresponding to a total luminosity of 704.0 pb^{-1}. Combining all final states in W-pair production, the mass and total decay width of the W boson are determined to be $M_W = 80.398 \pm 0.048$ (*stat.*) $\pm$ 0.050 (*syst.*) GeV and $\Gamma_W = 2.24 \pm 0.11$ (*stat.*) $\pm$ 0.15 (*syst.*) GeV, respectively. These results are preliminary.

Submitted to the 31^{st} *International Conference on High Energy Physics*
Amsterdam, Netherlands, 24-31 July 2002.

1 Introduction

For the 2000 data taking period, the centre-of-mass energy, $\sqrt{s}$, of the e^+e^- collider LEP at CERN was increased up to 208 GeV. This energy is well above the kinematic threshold of W-boson pair production, $e^+e^- \to W^+W^-$.

Analysis of W-pair production yields important knowledge about the Standard Model of electroweak interactions [1] through the measurements of the mass, M_W, and the total decay width, Γ_W, of the W boson [2]. These parameters were initially measured at $p\bar{p}$ colliders [3, 4].

First direct measurements of M_W in e^+e^- collisions were derived from total cross section measurements [5–9], mainly at the kinematic threshold of the reaction $e^+e^- \to W^+W^-$, $\sqrt{s} =$ 161 GeV, where the dependence of the W-pair cross section on the W-boson mass is largest. At centre-of-mass energies well above the kinematic threshold, the mass and also the total width of the W boson are determined by analysing the invariant mass of the W-boson decay products [7–11].

We report on the determination of the mass and the total width of the W boson. The analysis is based on the data sample collected in the year 2000 for centre-of-mass energies between 205 GeV and 208 GeV corresponding to an integrated luminosity of 217.3 pb^{-1}. The invariant mass distributions of 2521 W-pair events selected at these energies are analysed to determine M_W and Γ_W. The results based on the 2000 data are combined with our previous measurements at centre-of-mass energies between 161 GeV and 202 GeV [5,6,10–12]. All results based on data collected in 1998-2000 at $\sqrt{s} = 189 - 208$ GeV are preliminary.

2 Analysis of Four-Fermion Production

During the 2000 run the L3 detector [13] collected integrated luminosities of 78.9 pb^{-1}, 129.8 pb^{-1} and 8.5 pb^{-1}, at centre-of-mass energies of 204.82 GeV, 206.48 GeV and 208.00 GeV where these energies are known to $\pm$0.05 GeV [14]. The three data samples are collectively referred to as 2000 data in the following.

The W boson decays into a quark-antiquark pair, such as $W^- \to \bar{u}d$ or $\bar{c}s$, or a lepton-antilepton pair, $W^- \to \ell^-\bar{\nu}_\ell$ ($\ell = e, \mu, \tau$); in the following denoted as qq, $\ell\nu$ or ff in general for both W^+ and W^- decays. Four-fermion final states expected in W-pair production are $\ell\nu\ell\nu(\gamma)$, $qq\ell\nu(\gamma)$, and $qqqq(\gamma)$, where (γ) indicates the possible presence of radiative photons.

The following Monte Carlo event generators are used to simulate the signal and background reactions: KORALW [15] and HERWIG [16] ($e^+e^- \to WW \to ffff(\gamma)$); EXCALIBUR [17] ($e^+e^- \to ffff(\gamma)$); PYTHIA [18] and KK [19] ($e^+e^- \to q\bar{q}(\gamma)$); PYTHIA [18] ($e^+e^- \to ZZ(\gamma)$); KORALZ [20] and KK [19] ($e^+e^- \to \mu^+\mu^-(\gamma),\ \tau^+\tau^-(\gamma)$); BHAGENE3 [21], BHWIDE [22] and TEEGG [23] ($e^+e^- \to e^+e^-(\gamma)$); DIAG36 [24] and LEP4F [25] (leptonic two-photon collisions); PHOJET [26] (hadronic two-photon collisions). The response of the L3 detector is modelled with the GEANT [27] detector simulation program which includes the effects of energy loss, multiple scattering and showering in the detector material.

The selections of the four-fermion final states are described in detail in Reference 28. These analyses reconstruct the visible fermions in the final state, *i.e.*, electrons, muons, τ jets corresponding to the visible τ decay products, and hadronic jets corresponding to quarks. In order to select a pure sample of $qqqq$ events, the cut of 0.8 on the neural-network output described in the $qqqq$ cross-section analysis is applied [28]. Kinematic constraints as discussed below are then imposed to improve the resolution in the measured fermion energies and angles and to determine those not measured. The invariant mass of the W boson is obtained from its decay products.

The mass and the width of the W boson are determined by comparing samples of Monte Carlo events to the data. A reweighting procedure is applied to construct Monte Carlo samples corresponding to different mass and width values. Using this method, effects of selection and resolution are automatically taken into account.

3 Event Reconstruction imposing Kinematic Constraints

The final states $qqe\nu$, $qq\mu\nu$ and $qqqq$ contain at most one primary unmeasured neutrino. For each event a kinematic fit is performed in order to determine energy, E_f, polar angle, θ_f, and azimuthal angle, ϕ_f, for all four fermions, f, in the final state. The kinematic fit adjusts the measurements of these quantities for the visible fermions according to their experimental resolutions to satisfy the constraints imposed, thus improving their resolution.

Four-momentum conservation and equal mass of the two W bosons are imposed as constraints, allowing the determination of the momentum vector of the unmeasured neutrino. For the energy constraint, the exact centre-of-mass energies as given in the previous section are used. For hadronic jets, the velocity $\beta_f = |\vec{p}_f|/E_f$ of the jet is fixed to its measured value as systematic effects cancel in the ratio. For $qqe\nu$ and $qq\mu\nu$ events, this yields a two-constraint (2C) kinematic fit, whereas for $qqqq$ events it is a five-constraint (5C) kinematic fit.

Events with badly reconstructed hadronic jets are rejected by requiring that the probability of the kinematic fit exceeds 5%. The kinematic fit mainly improves the energy resolution and less the angular resolution. The resolutions in average invariant mass, m_{inv}, typically improve by a factor of four for $qqe\nu$ and $qq\mu\nu$ events and a factor of six for $qqqq$ events.

For $qq\tau\nu$ events, the decay products of the leptonically decaying W boson contain at least two unmeasured neutrinos in the final state. Therefore only the hadronically decaying W boson is used in the invariant mass reconstruction. The energies of the two hadronic jets are rescaled by a common factor so that the sum of their energies equals half the centre-of-mass energy, thus imposing equal mass of the two W bosons. The rescaling improves the resolution in invariant mass by nearly a factor of four. Since invariant masses of W bosons in $\ell\nu\ell\nu$ events cannot be reconstructed as the decay of both W bosons involves neutrinos, $\ell\nu\ell\nu$ events are not used in the analysis for W mass and width.

4 Fitting Method for Mass and Width

The fitting procedure uses the maximum likelihood method to extract values and errors of the W-boson mass M_{W}, and the total width Γ_{W}, denoted as Ψ for short in the following. In fits to determine M_{W} only, the Standard Model relation $\Gamma_{\mathrm{W}} = 3G_{\mathrm{F}}M_{\mathrm{W}}^3/(2\sqrt{2}\pi)(1+2\alpha_{\mathrm{S}}/(3\pi))$ [29] is imposed. Otherwise, M_{W} and Γ_{W} are treated as independent quantities.

The kinematic fit imposing the equal-mass constraint determines the weighted average of the two invariant W masses in an event, m_{inv}, which is considered in the fit for mass and width. The total likelihood is the product of the normalised differential cross section, $L(m_{\mathrm{inv}}, \Psi)$, evaluated for all data events. For a given four-fermion final state i, one has:

$$L_i(m_{\mathrm{inv}}, \Psi) \;=\; \frac{1}{f_i(\Psi)\sigma_i(\Psi) + \sigma_i^{\mathrm{BG}}} \left[f_i(\Psi) \frac{\mathrm{d}\sigma_i(m_{\mathrm{inv}}, \Psi)}{\mathrm{d}m_{\mathrm{inv}}} + \frac{\mathrm{d}\sigma_i^{\mathrm{BG}}(m_{\mathrm{inv}})}{\mathrm{d}m_{\mathrm{inv}}} \right], \qquad (1)$$

where σ_i and σ_i^{BG} are the accepted signal and background cross sections and $f_i(\Psi)$ a factor calculated such that the sum of accepted background and reweighted accepted signal cross section coincides with the measured cross section. This way mass and width are determined from the shape of the invariant mass distribution only. The total and differential cross sections of the accepted background are independent of the parameters Ψ of interest. They are taken from Monte Carlo simulations.

The total and differential signal cross sections depend on Ψ. For values Ψ_{fit} varied during the fitting procedure, these cross sections are determined by a reweighting procedure applied to Monte Carlo events originally generated with parameter values Ψ_{gen}. The event weights R_i are given by the ratio:

$$R_i(p_1, p_2, p_3, p_4, k_\gamma, \Psi_{\mathrm{fit}}, \Psi_{\mathrm{gen}}) \quad = \quad \frac{\left|\mathcal{M}_i^{\mathrm{4F}}(p_1, p_2, p_3, p_4, k_\gamma, \Psi_{\mathrm{fit}})\right|^2}{\left|\mathcal{M}_i^{\mathrm{CC03}}(p_1, p_2, p_3, p_4, k_\gamma, \Psi_{\mathrm{gen}})\right|^2}\,, \tag{2}$$

where $\mathcal{M}_i$ is the matrix element of the four-fermion final state i. The matrix elements are calculated for the generated four-vectors, $(p_1, p_2, p_3, p_4, k_\gamma)$, of the four fermions and any radiative photons in the event. Since the Monte Carlo sample used for reweighting is based on the three Feynman graphs in W-pair production (CC03 [29–31]), the matrix element in the denominator is calculated using only CC03 graphs. The matrix element in the numerator is based on all tree-level graphs contributing to the four-fermion final state i. The calculation of matrix elements is done with the EXCALIBUR [17] event generator.

The total accepted signal cross section for a given set of parameters Ψ_{fit} is then:

$$\sigma_i(\Psi_{\mathrm{fit}}) \quad = \quad \frac{\sigma_i^{\mathrm{gen}}}{N_i^{\mathrm{gen}}} \cdot \sum_j R_i(j, \Psi_{\mathrm{fit}}, \Psi_{\mathrm{gen}})\,, \tag{3}$$

where σ_i^{gen} denotes the cross section corresponding to the total Monte Carlo sample containing N_i^{gen} events. The sum extends over all Monte Carlo events j accepted by the event selection.

Based on the sample of reweighted events, the box method [32] is used to obtain the accepted differential signal cross section in reconstructed invariant mass m_{inv}. This method takes detector and selection effects as well as Ψ-dependent changes of efficiencies and purities properly into account.

In the box method, the accepted differential cross section is determined by averaging Monte Carlo events inside a m_{inv}-bin centred around each data event. The size of the bin considered is limited by the requirement of including a minimum of 100 and no more than 1000 Monte Carlo events. The bin sizes are always smaller than ± 250 MeV around m_{inv} and decrease to about ± 30 MeV at the peak of the invariant mass distribution. In case of background Monte Carlo the bin size is chosen to be ± 1 GeV.

The fit procedure described above determines the parameters without any bias as long as the Monte Carlo describes photon radiation and detector effects such as resolution and acceptance functions correctly. By fitting large Monte Carlo samples, typically a hundred times the data, the fitting procedure is tested to high accuracy. The fits reproduce well the values of the parameters of the large Monte Carlo samples being fitted. Also, the fit results do not depend on the values of the parameters Ψ_{gen} of the Monte Carlo sample subject to the reweighting procedure.

The reliability of the errors given by the fit is tested by fitting for each final state several hundred small Monte Carlo samples, each the size of the data samples. The width of the distribution of the fitted central values agrees well with the mean of the distribution of the fitted errors.

5 Mass and Total Width of the W Boson

Based on the data collected during 2000, the mass of the W boson is determined for each of the final states $qqe\nu$, $qq\mu\nu$, $qq\tau\nu$ and $qqqq$ in separate maximum likelihood fits. For mass fits in the $qqqq$ channel, the pairing algorithm to assign jets to W bosons used in the event selection [6,28,33–35] is changed. The pairing yielding the highest likelihood in the 5C kinematic fit is chosen. The fraction of correct pairings is reduced to 65% for the best combination and it is 23% for the second best combination. However, the signal-to-background ratio in the relevant signal region around $m_{\mathrm{inv}} \approx 80$ GeV is improved. The loss of correct pairings is recovered by including the pairing with the second highest likelihood as an additional distribution. Monte-Carlo studies show that the two values for M_{W} obtained from fitting separately the distributions of the best and the second best pairing have a correlation of $(0.1 \pm 1.4)\%$, which is negligible.

The observed invariant mass distributions together with the fit results for the semileptonic final states are shown in Figure 1. The distributions of the first and second pairing in $qqqq$ events are shown in Figure 2, while the distribution summed over all final states and both $qqqq$ pairings is shown in Figure 3. Combined results are determined by averaging the results of individual channels taking statistical and systematic errors into account. The results of fits for M_{W} are summarised in Table 1. The observed statistical errors agree with the statistical errors expected for the size of the data samples used.

6 Systematic Effects

The systematic errors on the fitted W mass and width are summarised in Table 3. They arise from various sources and are divided into systematic errors correlated between final states and systematic errors uncorrelated between final states.

6.1 Correlated Errors

The beam energy of LEP is known with an accuracy of 25 MeV for the 2000 data [14]. The relative error on M_{W} is given by the relative error on the LEP beam energy, while the width is less affected. The spread in centre-of-mass energy of about 0.2 GeV adds in quadrature to detector resolution and total width of the W boson and is thus negligible.

Systematic uncertainties due to incomplete simulations of initial-state radiation (ISR) are estimated by comparing the Monte Carlo generators KORALW and EXCALIBUR implementing different QED radiation schemes. For final-state radiation (FSR), events with FSR simulation are compared to events without any FSR and a third of the difference is taken as a systematic error.

The systematic error for the jet measurement is assigned from varying the jet energy scale by 0.1 GeV, smearing the jet energies by 1% and smearing the jet positions by 0.5°. These variations are consistent with a study of hadronic $q\bar{q}(\gamma)$ events collected at the Z pole and at higher centre-of-mass energies. Effects due to fragmentation are determined by comparing signal events simulated at $\sqrt{s} = 189$ GeV using string fragmentation as implemented in the JETSET Monte Carlo program and cluster fragmentation as implemented in the HERWIG Monte Carlo program to simulate the hadronisation process. In both fragmentation models the decay of unstable hadronic particles is simulated according to the JETSET decay table.

The fitting method itself is tested by fitting to various Monte Carlo samples generated with known values for M_{W} and Γ_{W}, varying over a range of ± 0.5 GeV. The systematic error due to the fitting method includes the effects due to different procedures for reweighting and choice of technical parameters such as box size and occupancy.

Limited Monte Carlo statistics introduces a tendency of the method to have a slope of the linear function relating fitted mass to generated mass less than one. All Monte Carlo samples, approximately 1.2 million events, are used in the reweighting procedure to minimise this effect when fitting data. Fitting several Monte Carlo samples and using the remaining Monte Carlo as reference the non-linearity is found to be negligible.

6.2 Uncorrelated Errors

The systematic error due to the size of the signal Monte Carlo sample used for reweighting is estimated by dividing it into N parts of equal size, N between 2 and 100, and making N fits to the same data sample. The spread of the fit results, divided by the square root of N-1, is found to be independent of N and yields the systematic error due to Monte Carlo statistics.

Selection effects are estimated by varying the cut on the probability of the kinematic fit and the interval of reconstructed invariant masses being fitted. Effects due to background are determined by varying both the total accepted background cross section within its error as evaluated for the cross section measurement as well as the shape of the invariant mass spectrum arising from the background.

For $qqqq$ events, strong final state interactions (FSI) between the hadronic systems of the two decaying W bosons due to effects of colour reconnection [36] or Bose-Einstein correlations [37] may affect the mass reconstruction. In both cases, possible effects are estimated by comparing signal simulations at 189 GeV centre-of-mass energy including and excluding the modelling of such effects assigning the maximal mass difference found as systematic error.

In case of colour reconnection (CR) a dedicated study of reconnection effects in the particle flow between jets in $qqqq$ events [38] shows that data are consistent with no or a small CR effect. In particular, an upper limit on the CR parameter is set in the framework of the CR model SK I [39] as implemented in PYTHIA 5.7. This limit corresponds to a maximal reconnection probability of about 46% at 189 GeV, which translates into a maximal mass shift of less than 40 MeV [1)]. However, the particle flow analysis is found to be insensitive to CR effects implemented in other models like ARIADNE type II [40] and HERWIG. Although the ARIADNE II model has no effect on the particle flow it leads to a significant shift of 50 ± 9 MeV on the W mass. HERWIG CR introduces a mass bias of 35 ± 9 MeV. Other scenarios studied in the mass analysis are: the models SK II and II' [39], and the GH [41] model, implemented in PYTHIA 5.7 and adjusted to yield 30% reconnection probability. For all analysed models a W mass shift smaller than for ARIADNE II is observed, so that 50 MeV is finally taken as systematic uncertainty.

Our measurement [42] of Bose-Einstein (BE) correlations indicates that BE correlations in hadronic W decays are very similar to those in Z decays to light quarks. Furthermore, BE correlations between hadrons from different W bosons are disfavoured and limited to at most a quarter of the strength as simulated in BE0 and BE32 models which are implemented in JETSET and PYTHIA 5.7 [43]. Since all our previous mass measurements were performed under the assumption of full inter-W correlations, the results obtained in the $qqqq$ channel are reevaluated for the assumption of vanishing inter-W correlations. The systematic error includes the effect of the remaining allowed strength of inter-W correlations.

[1)]The W mass biases due to the SK I, ARIADNE II and HERWIG CR models are determined from LEP common Monte Carlo samples of KORALW events produced at 189 GeV.

For $qqe\nu$ and $qq\mu\nu$ events, the reconstruction of the lepton energy and angles also affects the invariant mass reconstruction. In analogy to hadronic jets, control samples of $\ell^+\ell^-(\gamma)$ events selected at the Z pole are used to cross check the reconstruction of leptons. Energy scales and resolutions are varied within their errors and the resulting effect on W mass and width is quoted as a systematic error.

7 Results

The results on M_{W} determined for 2000 data in the $qqe\nu$, $qq\mu\nu$, and $qq\tau\nu$ final states are in good agreement with each other, as shown in Table 1. They are averaged taking statistical and systematic errors including correlations into account, and compared to the result on M_{W} determined in the $qqqq$ final state, also shown in Table 1. The observed invariant mass distributions of each individual channel as well as their summed distribution are shown in Figures 1, 2, and 3 together with the expectations based on the obtained W-mass values.

Combining the results from 2000 data with the ones determined at lower centre-of-mass energies of $172 - 202$ GeV yields [12]:

$$\begin{aligned} M_{\mathrm{W}}(qq\ell\nu) &= 80.314 \pm 0.074\ (stat.) \pm 0.045\ (syst.)\ \mathrm{GeV} & (4) \\ M_{\mathrm{W}}(qqqq) &= 80.478 \pm 0.063\ (stat.) \pm 0.069\ (syst.)\ \mathrm{GeV}\,. & (5) \end{aligned}$$

These two results are correlated having a correlation coefficient of 21%. The quoted systematic error on the mass derived from $qqqq$ events contains a contribution from possible strong FSI effects. The same numerical results are obtained when the $qq\ell\nu$ and $qqqq$ data are analysed separately neglecting correlations between them.

The difference between M_{W} in $qq\ell\nu$ and $qqqq$ events is determined to be:

$$\Delta M_{\mathrm{W}} = M_{\mathrm{W}}(qqqq) - M_{\mathrm{W}}(qq\ell\nu) = 0.163 \pm 0.097\ (stat.) \pm 0.046\ (syst.)\ \mathrm{GeV}\,. \quad (6)$$

For the calculation of the systematic error on the mass difference, the systematic errors due to strong FSI are not included and errors from fragmentation are treated as uncorrelated between $qq\ell\nu$ and $qqqq$ final states. This causes ΔM_{W} not to be equal to the difference of the mass values given in eq(4) and eq(5).

Averaging the results on M_{W} obtained from the $qq\ell\nu$ and $qqqq$ event samples, including FSI errors and all correlations, yields:

$$M_{\mathrm{W}} = 80.389 \pm 0.048\ (stat.) \pm 0.051\ (syst.)\ \mathrm{GeV}\,. \quad (7)$$

By combining the direct reconstruction result with the one obtained from cross-section measurements at 161 GeV and 172 GeV, the mass of the W boson is measured to be:

$$M_{\mathrm{W}} = 80.398 \pm 0.048\ (stat.) \pm 0.050\ (syst.)\ \mathrm{GeV}\,. \quad (8)$$

The total width of the W boson is determined in fits to both M_{W} and Γ_{W}. The obtained values of M_{W} are the same as before within 10 MeV while the error on the mass is unchanged as shown in Table 2 for 2000 data. For all final states combined the result is:

$$\Gamma_{\mathrm{W}} = 2.21 \pm 0.21\ (stat.) \pm 0.17\ (syst.)\ \mathrm{GeV}\,. \quad (9)$$

Averaging this result with the width measurements at $172 - 202$ GeV yields [12]:

$$\Gamma_{\mathrm{W}} = 2.24 \pm 0.11\ (stat.) \pm 0.15 (syst.)\ \mathrm{GeV}\,, \quad (10)$$

with a correlation coefficient of 0.6% between M_{W} and Γ_{W} as shown in Figure 4. Our result on Γ_{W} is in good agreement with the indirect measurement at $\mathrm{p\bar{p}}$ colliders, 2.17 ± 0.05 GeV [4], and measurements at LEP [7–9]. It also agrees well with the Standard Model expectation, 2.10 GeV, calculated for the current world-average W mass [44].

This direct determination of M_{W} is in good agreement with the direct determination of M_{W} at $\mathrm{p\bar{p}}$ colliders [3] and at LEP at lower centre-of-mass energies [7–9]. It also agrees with our indirect determination of M_{W} at the Z peak, $M_{\mathrm{W}} = 80.523 \pm 0.079$ GeV [45], testing the Standard Model at the level of its electroweak corrections.

8 Acknowledgements

We wish to congratulate the CERN accelerator divisions for the successful operation of the LEP machine and to express our gratitude for its good performance. We acknowledge with appreciation the effort of the engineers, technicians and support staff who have participated in the construction and maintenance of this experiment.

References

[1] S. L. Glashow, Nucl. Phys. **22** (1961) 579;
S. Weinberg, Phys. Rev. Lett. **19** (1967) 1264;
A. Salam, in *Elementary Particle Theory*, ed. N. Svartholm, Stockholm, Almquist and Wiksell (1968), 367.

[2] Z. Kunszt *et al.*, in *Physics at LEP 2*, Report CERN 96-01 (1996), eds G. Altarelli, T. Sjöstrand, F. Zwirner, Vol. 1, p. 141.

[3] The UA1 Collaboration, C. Albajar *et al.*, Z. Phys. **C 44** (1989) 15;
The UA2 Collaboration, J. Alitti *et al.*, Phys. Lett. **B 241** (1990) 150; Phys. Lett. **B 276** (1992) 354;
The CDF Collaboration, F. Abe *et al.*, Phys. Rev. Lett. **65** (1990) 2243; Phys. Rev. **D 43** (1991) 2070; Phys. Rev. Lett. **75** (1995) 11; Phys. Rev. **D 52** (1995) 4784;
The DØ Collaboration, S. Abachi *et al.*, Phys. Rev. Lett. **77** (1996) 3309; B. Abbott *et al.*, Phys. Rev. **D 58** (1998) 012002; B. Abbott *et al.*, Phys. Rev. Lett. **80** (1998) 3008; B. Abbott *et al.*, Phys. Rev. **D 58** (1998) 092003.

[4] The UA1 Collaboration, C. Albajar *et al.*, Phys. Lett. **B 253** (1991) 503;
The UA2 Collaboration, J. Alitti *et al.*, Phys. Lett. **B 276** (1992) 365;
The CDF Collaboration, F. Abe *et al.*, Phys. Rev. Lett. **74** (1995) 341; Phys. Rev. **D 52** (1995) 2624;
The DØ Collaboration, S. Abachi *et al.*, Phys. Rev. Lett. **75** (1995) 1456.

[5] The L3 Collaboration, M. Acciarri *et al.*, Phys. Lett. **B 398** (1997) 223.

[6] The L3 Collaboration, M. Acciarri *et al.*, Phys. Lett. **B 407** (1997) 419.

[7] The ALEPH Collaboration, R. Barate *et al.*, Eur. Phys. J. **C 17** (2000) 241.

[8] The DELPHI Collaboration, P. Abreu *et al.*, Phys. Lett. **B 511** (2001) 159.

[9] The OPAL Collaboration, G. Abbiendi *et al.*, Phys. Lett. **B 507** (2001) 29.

[10] The L3 Collaboration, M. Acciarri *et al.*, Phys. Lett. **B 413** (1997) 176.

[11] The L3 Collaboration, M. Acciarri *et al.*, Phys. Lett. **B 454** (1999) 386.

[12] The W-Physics Analysis Group of the L3 Collaboration,
Preliminary Results on the Measurement of the Mass and Width of the W Boson at LEP, L3 Note 2575, June 2000.

[13] The L3 Collaboration, B. Adeva *et al.*, Nucl. Instr. and Meth. **A 289** (1990) 35;
M. Chemarin *et al.*, Nucl. Instr. and Meth. **A 349** (1994) 345;
M. Acciarri *et al.*, Nucl. Instr. and Meth. **A 351** (1994) 300;
G. Basti *et al.*, Nucl. Instr. and Meth. **A 374** (1996) 293;
I.C. Brock *et al.*, Nucl. Instr. and Meth. **A 381** (1996) 236;
A. Adam *et al.*, Nucl. Instr. and Meth. **A 383** (1996) 342.

[14] LEP Energy Working Group, Internal Note LEPEWG 01/01, March 2001.

[15] KORALW version 1.33 is used.
M. Skrzypek, S. Jadach, W. Placzek and Z. Wąs, Comp. Phys. Comm. **94** (1996) 216;
M. Skrzypek, S. Jadach, M. Martinez, W. Placzek and Z. Wąs, Phys. Lett. **B 372** (1996) 289.

[16] HERWIG version 5.9 is used.
G. Marchesini and B. Webber, Nucl. Phys. **B 310** (1988) 461;
I.G. Knowles, Nucl. Phys. **B 310** (1988) 571;
G. Marchesini *et al.*, Comp. Phys. Comm. **67** (1992) 465.

[17] F.A. Berends, R. Kleiss and R. Pittau, Nucl. Phys. **B 424** (1994) 308; Nucl. Phys. **B 426** (1994) 344; Nucl. Phys. (Proc. Suppl.) **B 37** (1994) 163;
R. Kleiss and R. Pittau, Comp. Phys. Comm. **83** (1994) 141;
R. Pittau, Phys. Lett. **B 335** (1994) 490.

[18] PYTHIA version 5.722 is used.
T. Sjöstrand, *PYTHIA 5.7 and JETSET 7.4 Physics and Manual*,
CERN-TH/7112/93 (1993), revised August 1995; Comp. Phys. Comm. **82** (1994) 74.

[19] KK version 4.12 is used.
S. Jadach, B. F. L. Ward and Z. Wąs, *The precision Monte Carlo event generator KK for two-fermion final states in* e^+e^- *collisions*, CERN-TH/235/99.

[20] KORALZ version 4.02 is used.
S. Jadach, B. F. L. Ward and Z. Wąs, Comp. Phys. Comm. **79** (1994) 503.

[21] J.H. Field, Phys. Lett. **B 323** (1994) 432;
J.H. Field and T. Riemann, Comp. Phys. Comm. **94** (1996) 53.

[22] BHWIDE version 1.01 is used.
S. Jadach, W. Placzek, B.F.L. Ward, Phys. Rev. **D 40** (1989) 3582, Comp. Phys. Comm. **70** (1992) 305, Phys. Lett. **B 390** (1997) 298.

[23] D. Karlen, Nucl. Phys. **B 289** (1987) 23.

[24] F. A. Berends, P. H. Daverfeldt and R. Kleiss, Nucl. Phys. **B 253** (1985) 441.

[25] J.A.M. Vermaseren, J. Smith and G. Grammer Jr, Phys. Rev. **D 19** (1979) 137;
J.A.M. Vermaseren, Nucl. Phys. **B 229** (1983) 347.

[26] PHOJET version 1.05 is used.
R. Engel, Z. Phys. **C 66** (1995) 203; R. Engel and J. Ranft, Phys. Rev. **D 54** (1996) 4244.

[27] The L3 detector simulation is based on GEANT Version 3.15.
R. Brun *et al.*, *GEANT 3*, CERN-DD/EE/84-1 (Revised), 1987.
The GHEISHA program (H. Fesefeldt, RWTH Aachen Report PITHA 85/02 (1985)) is used to simulate hadronic interactions.

[28] The W-Physics Analysis Group of the L3 Collaboration,
Preliminary Results on the Measurement of W-Pair Cross Sections in e^+e^- *Interactions at* $\sqrt{s}$ *= 205-208 GeV and W-Decay Branching Fractions*, L3 Note 2638, March 2001.

[29] W. Beenakker *et al.*, in *Physics at LEP 2*, Report CERN 96-01 (1996), eds G. Altarelli, T. Sjöstrand, F. Zwirner, Vol. 1, p. 79.

[30] D. Bardin *et al.*, Nucl. Phys. (Proc. Suppl.) **B 37** (1994) 148;
F.A. Berends *et al.*, Nucl. Phys. (Proc. Suppl.) **B 37** (1994) 163.

[31] D. Bardin *et al.*, in *Physics at LEP 2*, Report CERN 96-01 (1996), eds G. Altarelli, T. Sjöstrand, F. Zwirner, Vol. 2, p. 3.

[32] D.M. Schmidt, R.J. Morrison and M.S. Witherell, Nucl. Instr. and Meth. **A 328** (1993) 547.

[33] The L3 Collaboration, M. Acciarri *et al.*, Phys. Lett. **B 436** (1998) 437.

[34] The L3 Collaboration, M. Acciarri *et al.*, Phys. Lett. **B 496** (2000) 19.

[35] The W-Physics Analysis Group of the L3 Collaboration,
Preliminary Results on the Measurement of W-Pair Cross Sections in e^+e^- *Interactions at* $\sqrt{s}$ *= 192-202 GeV and W-Decay Branching Fractions*, L3 Note 2514, March 2000.

[36] G. Gustafson, U. Petterson and P.M. Zerwas, Phys. Lett. **B 209** (1988) 90;
T. Sjöstrand and V.A. Khoze, Z. Phys. **C 62** (1994) 281, Phys. Rev. Lett. **72** (1994) 28;
E. Accomando, A. Ballestrero and E. Maina, Phys. Lett. **B 362** (1995) 141;
G. Gustaffson and J. Häkkinen, Z. Phys. **C 64** (1994) 659;
L. Lönnblad, Z. Phys. **C 70** (1996) 107;
J. Ellis and K. Geiger, Phys. Rev. **D 54** (1996) 1967, Phys. Lett. **B 404** (1997) 230;
V.A. Khoze and T. Sjöstrand, Eur. Phys. J. **C 6** (1999) 271
.

[37] L. Lönnblad and T. Sjöstrand, Phys. Lett. **B 351** (1995) 293;
S. Jadach and K. Zalewski, Acta Phys. Polon **B 28** (1997) 1363;
V. Kartvelishvili, R. Kvatadze and R. Møller, Phys. Lett. **B 408** (1997) 331;
K. Fialkowski and R. Wit, Z. Phys. **C 74** (1997) 145;
K. Fialkowski, R. Wit and J. Wosiek, Phys. Rev. **D 58** (1998) 094013;
L. Lönnblad and T. Sjöstrand, Eur. Phys. J. **C 2** (1998) 165.

[38] The W-Physics Analysis Group of the L3 Collaboration,
Search for Colour Reconnection Effects in $e^+e^- \to W^+W^- \to$ *hadrons through Particle-Flow Studies at* $\sqrt{s} = 189 - 209$GeV, L3 Note 2748, March 2002.

[39] T. Sjöstrand and V. Khoze, Z. Phys. **C 62** (1994) 281;
V. Khoze and T. Sjöstrand, Eur. Phys. J. **C 6** (1999) 271.

[40] ARIADNE version 4 revision 08 is used.
I. Lönnblad, Comp. Phys. Comm. **71** (1992) 15.

[41] G. Gustafson and J. Häkkinen, Z. Phys. **C 64** (1994) 659.

[42] The L3 Collaboration, M. Acciarri *et al.*, Phys. Lett. **B 493** (2000) 233.

[43] L. Lönnblad and T. Sjöstrand, Phys. Lett. **B 351** (1995) 293;
L. Lönnblad and T. Sjöstrand, Eur. Phys. J. **C 2** (1998) 165.

[44] D. E. Groom *et al.*, *The 2000 Review of Particle Physics*, Eur. Phys. J. **C 16** (2000) 1.

[45] The L3 Collaboration, M. Acciarri *et al.*, Eur. Phys. J. **C 16** (2000) 1.

Process	Events	Mass of the W Boson	Expected Stat.
	205 – 208 GeV	M_{W} [GeV]	Error [GeV]
$\mathrm{e^+e^-} \to qqe\nu(\gamma)$	352	$80.58 \pm 0.19 \pm 0.05$	± 0.18
$\mathrm{e^+e^-} \to qq\mu\nu(\gamma)$	327	$80.05 \pm 0.23 \pm 0.06$	± 0.22
$\mathrm{e^+e^-} \to qq\tau\nu(\gamma)$	450	$80.69 \pm 0.36 \pm 0.08$	± 0.30
$\mathrm{e^+e^-} \to qq\ell\nu(\gamma)$	1129	$80.41 \pm 0.14 \pm 0.05$	± 0.12
$\mathrm{e^+e^-} \to qqqq(\gamma)$	1392	$80.51 \pm 0.11 \pm 0.07$	± 0.11
$\mathrm{e^+e^-} \to ffff(\gamma)$	2521	$80.47 \pm 0.08 \pm 0.06$	± 0.08

Table 1: Number of events used in the analysis and results on the mass of the W boson, M_{W}, for the data collected at $205-208$ GeV. The first error is statistical and the second systematic. Also shown is the statistical error expected for the size of the data sample analysed. There is a small overlap of events between channels.

Process	Mass of the W Boson	Total Decay Width	Correlation
	M_{W} [GeV]	Γ_{W} [GeV]	Coefficient
$\mathrm{e^+e^-} \to qq\ell\nu(\gamma)$	$80.41 \pm 0.14 \pm 0.05$	$2.51 \pm 0.34 \pm 0.14$	-0.05
$\mathrm{e^+e^-} \to qqqq(\gamma)$	$80.52 \pm 0.11 \pm 0.07$	$1.93 \pm 0.27 \pm 0.24$	-0.10
$\mathrm{e^+e^-} \to ffff(\gamma)$	$80.47 \pm 0.09 \pm 0.06$	$2.15 \pm 0.21 \pm 0.17$	-0.08

Table 2: Results on the mass of the W boson, M_{W}, and its total decay width, Γ_{W}, obtained from a fit to both quantities using data collected at $205-208$ GeV. The first error is statistical and the second systematic. Also shown is the correlation coefficient between M_{W} and Γ_{W}.

Systematic Errors on M_W [MeV] at $\sqrt{s} = 205 - 208$ GeV				
Error Source	Final State			
	$qqe\nu$	$qq\mu\nu$	$qq\tau\nu$	$qqqq$
LEP Energy	20	20	20	20
ISR	15	15	15	10
FSR	10	10	10	5
Jet Measurement	10	25	25	20
Fragmentation	30	30	30	30
Fitting Method	15	15	15	15
Total Correlated	44	50	50	45
MC Statistics	18	17	31	11
Colour Reconnection	—	—	—	50
Bose-Einstein Effects	—	—	—	20
Selection	10	10	10	10
Background	5	5	45	15
Lepton Measurement	15	15	—	—
Total Uncorrelated	26	25	56	58
Total Systematic	51	56	75	73

Table 3: Systematic errors in the determination of M_W for the different final states used for the measurement at $\sqrt{s} = 205 - 208$ GeV. The contributions listed in the upper part of the table are treated as correlated when combining different final states. Total errors are obtained by adding the individual contributions in quadrature.

Systematic Errors on Γ_W [MeV] at $\sqrt{s} = 205 - 208$ GeV		
Error Source	Final State	
	$qq\ell\nu$	$qqqq$
LEP Energy	14	14
ISR	25	15
FSR	15	10
Jet Measurement	80	15
Fragmentation and Decay	60	200
Fitting Method	25	25
Total Correlated	108	204
MC Statistics	63	29
Colour Reconnection	—	80
Bose-Einstein Effects	—	50
Selection	40	50
Background	35	40
Lepton Measurement	30	—
Total Uncorrelated	88	118
Total Systematic	139	235

Table 4: Systematic errors in the determination of Γ_W in $qq\ell\nu$ and $qqqq$ production. The contributions listed in the upper part of the table are treated as correlated when combining the two final states. The contributions listed in the lower part are treated as uncorrelated between channels. Total errors are obtained by adding the individual contributions in quadrature.

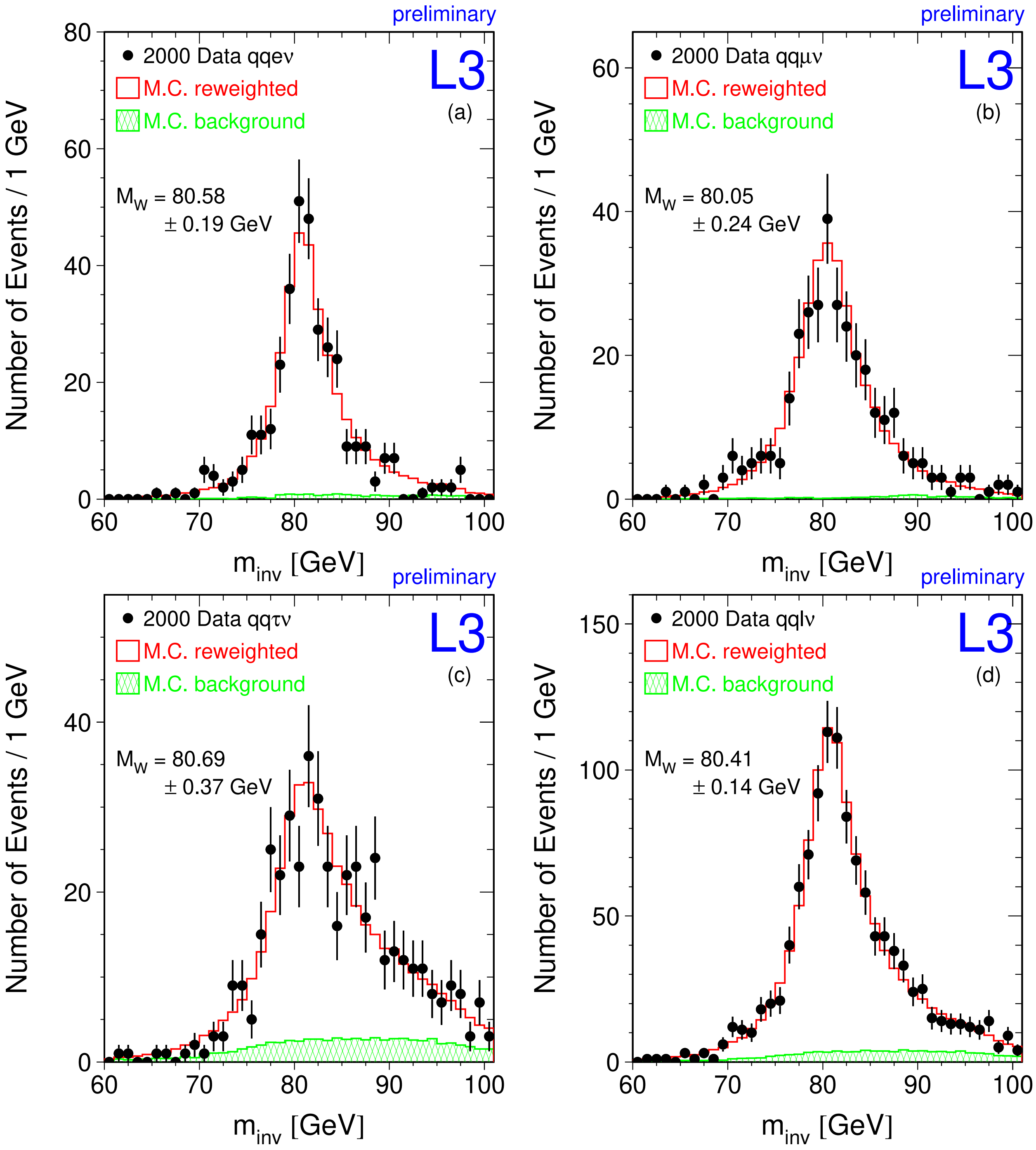

Figure 1: Distributions of reconstructed invariant mass, $m_{\rm inv}$, after applying the kinematic fit using the equal-mass constraint for events selected in the $205-208$ GeV data: (a) $qqe\nu$, (b) $qq\mu\nu$, (c) $qq\tau\nu$, (d) $qq\ell\nu$, combining $qqe\nu$, $qq\mu\nu$ and $qq\tau\nu$. The solid lines show the result of the fits of $M_{\rm W}$ to the indicated final states. The quoted error combines statistical and systematic errors in quadrature.

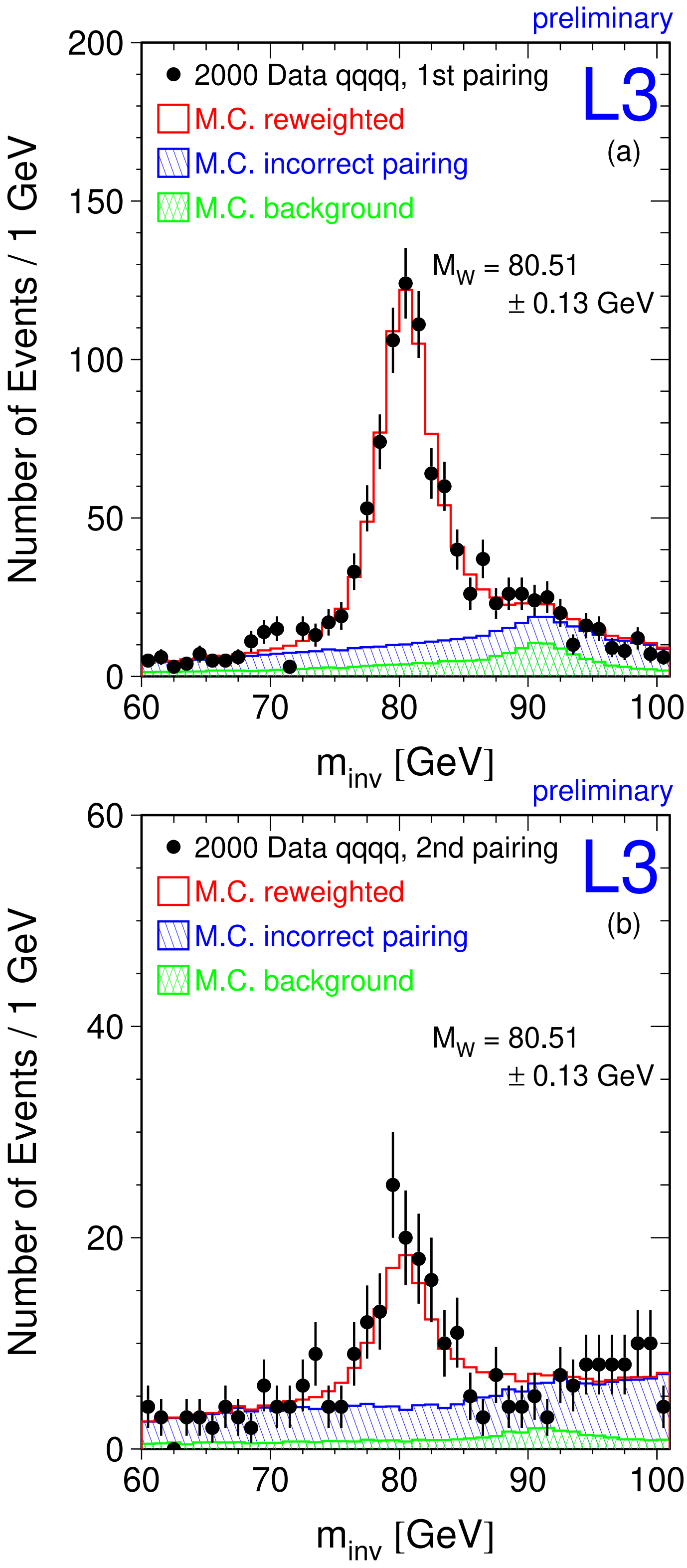

Figure 2: Distributions of reconstructed invariant mass, m_{inv}, after applying the kinematic fit using the equal-mass constraint for $qqqq$ events selected in the $205-208$ GeV data: (a) first pairing, (b) second pairing. The solid lines show the result of the fit of M_{W} to both pairings. The quoted error combines statistical and systematic errors in quadrature.

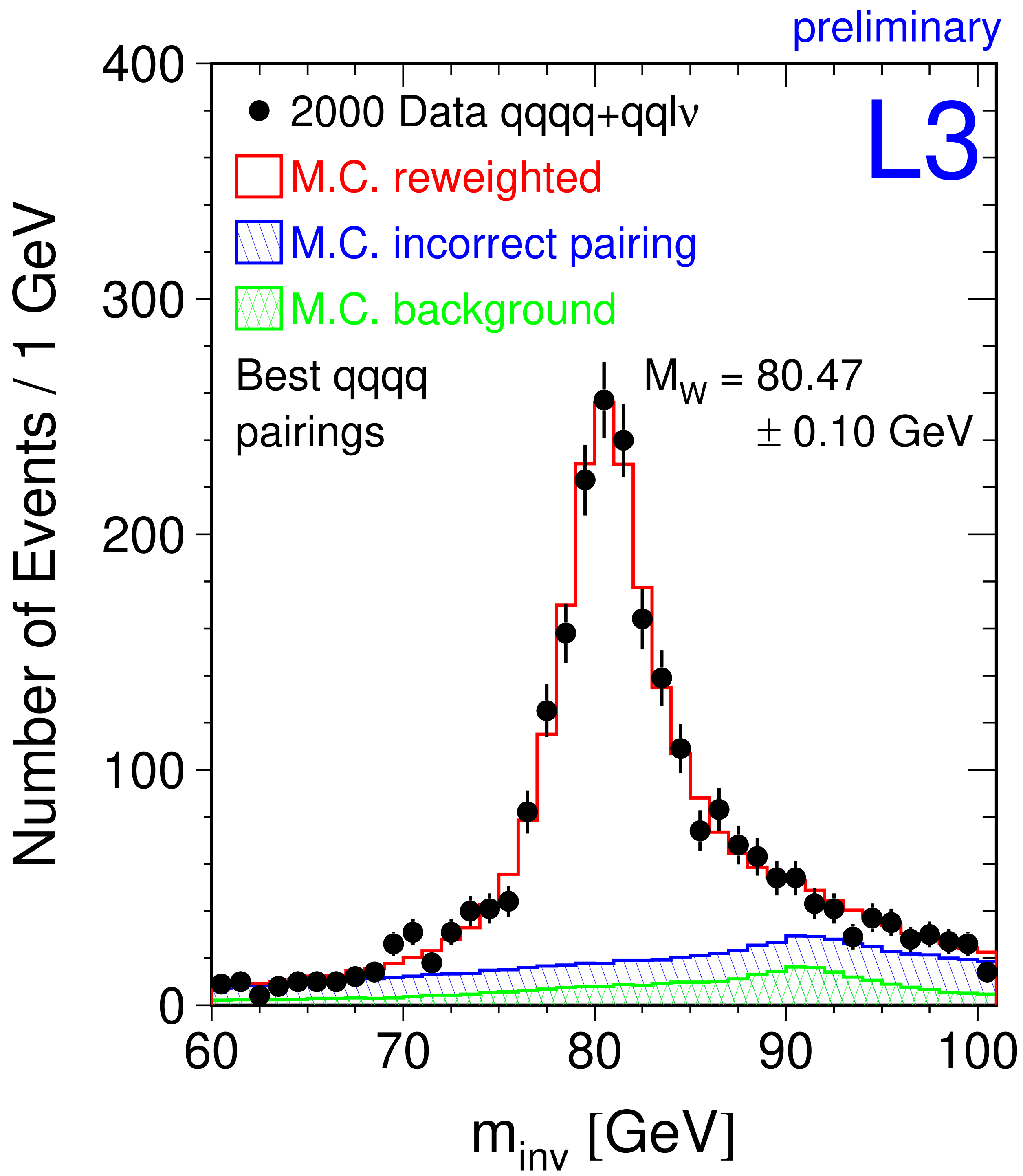

Figure 3: Distribution of reconstructed invariant mass, m_{inv}, after applying the kinematic fit using the equal-mass constraint for all W-pair events selected in the $205-208$ GeV data used for the mass analysis. For *qqqq* events, the two best pairings are included. The solid line shows the result of the fit of M_{W}. The quoted error combines statistical and systematic errors in quadrature.

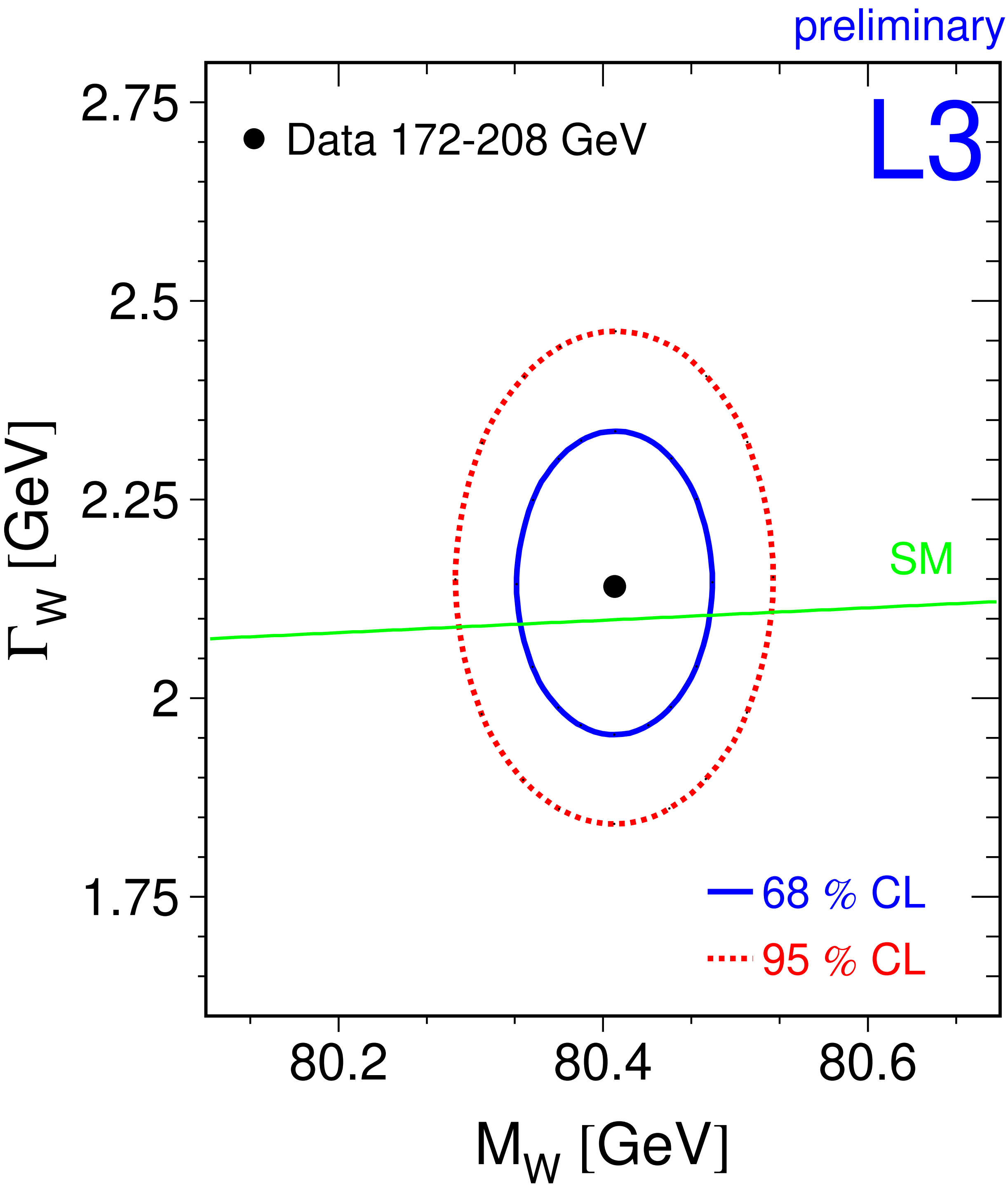

Figure 4: Contour curves of 68% and 95% probability in the $(M_\mathrm{W}, \Gamma_\mathrm{W})$ plane from a fit to the combined $172 - 208$ GeV data. Only statistical errors are taken into account. The point represents the central values of the fits. The Standard Model dependence of Γ_W on M_W is shown as the line.